Supporting Material

Vesicle fusion observed by content transfer across a tethered lipid bilayer

Robert J. Rawle[*], Bettina van Lengerich[*], Minsub Chung[*], Poul Martin Bendix[*†], and Steven G. Boxer[*]

**Department of Chemistry, Stanford University, Stanford, California 94305*

Corresponding Author:

Steven G. Boxer

(650) 723-4482; fax: (650) 723-4817

sboxer@stanford.edu

[†] Current address: Niels Bohr Institute, Blegdamsvej 17, 2100 Copenhagen, Denmark

SUPPLEMENTARY METHODS

Materials

Dioleoyl phosphatidylethanolamine (DOPE), Dioleoyl phosphatidylcholine (DOPC) and cholesterol (Chol) were purchased from Avanti Polar Lipids. Texas Red-1,2-dihexadecanoyl-*sn*-glycero-3-phosphoethanolamine (TR-DHPE), Oregon Green-1,2-dihexadecanoyl-*sn*-glycero-3-phosphoethanolamine (OG-DHPE), 1,1'-dioctadecyl-3,3,3',3'-tetramethylindocarbocyanine (DiI), and 1,1'-dioctadecyl-3,3,3',3'-tetramethylindodicarbocyanine (DiD) were purchased from Invitrogen. Sulforhodamine B and sucrose were purchased from Sigma-Aldrich and calcein was purchased from Alfa Aesar. Chloroform and methanol were obtained from Fischer. DNA-lipid conjugates were prepared as described previously (S3).

Fluorescence Microscopy

Epifluorescence and total internal reflectance fluorescence (TIRF) microscopy images were obtained on a Nikon Eclipse Ti-U inverted microscope with a 100x oil immersion objective (NA 1.49, Nikon). Two diode lasers (488 nm and 532 nm, Melles Griot) were set up to perform through-objective TIRF illumination. The typical laser power used in the single color content release experiments (488nm laser only) was 290 μW measured through the objective (not in TIR mode). For the two-color measurements of simultaneous lipid-mixing and content release, the laser powers were 510 μW for the 488 nm laser and 140 μW for the 532 nm laser, also measured through the objective. The laser intensity was distributed across an approximately 60 μm by 60 μm region at the sample plane and in TIRF mode the exact laser intensity at any given point in the sample will be a function of the vertical distance from the surface of the substrate as well as the angle of incidence of the laser. The fusion-to-tethered GUV and lipid-mixing-to-tethered patch experiments were acquired using epifluorescence illumination from a mercury arc lamp. Images and video streams were recorded using an Andor iXon897 CCD camera via the Metamorph software (version 7.6.4.0, MDS Analytical Technologies). A typical video stream for the SUV-to-tethered bilayer patch content transfer experiments was acquired for 6000 frames at 5.5 ms per frame and typical two-color videos of simultaneous lipid-mixing and content transfer were acquired at 15 ms per frame. Video streams for lipid-mixing only experiments (for lipid diffusion analysis) were acquired at 53 ms per frame. Several sequential video streams were acquired for most experiments. Integrated intensity time traces of fusion events in video streams were quantified using a homemade program in MATLAB (The MathWorks, Inc.).

Small Unilamellar Vesicle (SUV) Preparation

Lipid mixtures of 2:1:1 DOPC:DOPE:Chol with 2 mole % of lipid dyes as needed were made in chloroform, dried under a steady stream of nitrogen gas and then placed under vacuum for at least three hours. Dried lipid mixtures were resuspended in 10mM NaH_2PO_4 100mM Calcein buffer at pH 7.75 (~400mM NaOH added to achieve this pH) and then extruded through a polycarbonate membrane (Whatman, 50 nm or 100 nm pore size) at least 25 times using an Avanti mini-extruder. The appropriate volume of DNA-lipids (PolyA-lipid, Supplementary Table 1) in H_2O was then added to the SUV suspension in order to yield the desired mole % of DNA-lipids in each vesicle (typically

0.5-1.0 mole % was used, and typical volumes were ~0.5 μL DNA-lipid added to 20 μL SUV suspension). The SUV/DNA-lipid mixture was incubated at 4°C overnight in order to give sufficient time for the DNA-lipids to insert into the SUV bilayers. SUVs decorated with DNA-lipids were stored at 4°C and used within several days of extrusion. Immediately before a fusion experiment, the SUVs were purified from the free calcein dye on a CL-4B size exclusion column (Sigma) equilibrated with 10mM NaH_2PO_4 240mM NaCl buffer at pH 7.4.

Supplementary Table 1. Sequences and coupling orientations of DNA-lipids

Name	Sequence (5' to 3')
Sequence 1	lipid-5' TAG TAT TCA ACA TTT CCG TGT CGA 3'
Sequence 2	Alkyne-5' TCG ACA CGG AAA TGT TGA ATA CTA 3'
PolyT-lipid	lipid-5' TTT TTT TTT TTT TTT TTT TTT TTT 3'
PolyA-lipid	5' AAA AAA AAA AAA AAA AAA AAA AAA 3'-lipid

Giant Unilamellar Vesicle (GUV) Preparation by Gentle Hydration

The appropriate volumes of DNA-lipids in H_2O needed to yield 0.5 mole % in the final GUV mixture were added to a glass vial and thoroughly dried under a steady stream of nitrogen gas. For all GUVs in this study, two different DNA-lipids (0.5 mole% of each type) were utilized: Sequence 1 and PolyT-lipid in Supplementary Table 1. Sequence 1 was used to tether the GUV to the DNA surface, resulting in a membrane patch, and PolyT-lipid was used to mediate fusion with the SUVs.

The dried DNA-lipids were dissolved in 100 μL methanol followed by addition of 100 μL chloroform. To this solution was added 20 μL of 2:1:1 DOPC:DOPE:Chol dissolved in chloroform at 5 mg/mL, followed by the addition of 1.6 μL of 0.01 mg/mL OG-DHPE in chloroform (yielding 0.01 mole %). The solution was then dried under a steady stream of nitrogen gas and placed under vacuum for at least three hours. To the dried lipid/DNA-lipid mixture was added 2mL of 500 mM sucrose warmed to 37°C, and GUVs were formed by gentle hydration at 37°C with mild rocking overnight. The resultant GUVs were stored at 4°C and used within several days. Note that for DNA-tethered bilayer patch formation, the preparation of GUVs by gentle hydration works as well as electroformation, which was used in previous work (S1) and in the tethered GUV-based experiments described below. Also note that because DNA-lipids are included in the lipid mixture, we expect DNA to be displayed on both the outside and inside of the GUV and also on both sides of the DNA-tethered bilayers patch once formed. The non-hybridized single stranded DNA strands on the lower leaflet of the patch are not shown to reduce clutter in Figure 1 in the main text and in Figure S5 below.

Tethered Membrane Patch Formation and SUV-to-Membrane Patch Fusion Experiments

Immobilized DNA surfaces were prepared on glass coverslips inside a CoverWell perfusion chamber gasket (Invitrogen) using the click reaction as previously described (S1). The only alteration was the omission of the 150 mM Hepes/0.1% SDS/1x saline-sodium citrate rinse in order to avoid contamination of the surface with SDS, which might affect the fuseogenic properties of the membrane patches. Instead, the DNA

surface was thoroughly rinsed with 10mM NaH_2PO_4 240mM NaCl buffer at pH 7.4. The DNA-alkyne attached to the surface was Sequence 2 in Supplementary Table 1.

Following the prescribed cleaning protocol, the DNA surface was hydrated in the perfusion chamber gasket with 200 μL of 10mM NaH_2PO_4 240mM NaCl buffer at pH 7.4. 20 μL of GUV suspension was added to the hydrated surface and incubated for several minutes while being monitored by epifluorescence microscopy. When a sufficient number of tethered membrane patches were observed to have formed, the sample was rinsed at least 5 times with 250 μL of 10mM NaH_2PO_4 240mM NaCl buffer at pH 7.4 to remove non-tethered GUVs and lipid debris on tethered membrane patch surfaces.

An appropriately sized tethered membrane patch was then located on the microscope. To minimize edge effects, data was generally collected from only the central area of the patch. The small percentage of OG-DHPE membrane dye in the patch, used to locate the correct focal plane, was photobleached so as to not provide unwanted background during the fusion experiments. Several μL of diluted SUV suspension was then manually pipetted into the solution above the membrane patch. Docking and fusion were observed via epifluorescence or TIRF video microscopy.

2D AND 3D CONTENT DYE DIFFUSION MODELS AND DATA ANALYSIS

Our diffusion models were based on those performed by Weisshaar et al. (S2). According to this analysis, a content transfer or content leakage event is modeled as the release of all fluorophores from a point source either underneath the membrane patch into the quasi-2D 8 nm gap between the membrane patch and the substrate or above the membrane patch into bulk solution, which constitutes a 3D half-space. Following the Weisshaar et al. analysis, the absolute integrated fluorescence intensity within a cylindrical volume of radius R centered on the release point and height h can be calculated in cylindrical coordinates as

$$F(t) = A\int_0^R 2\pi\rho\, d\rho \int_0^h C(\rho,z,t)\,\phi_{rel}(\rho,z,t)\, I_{laser}(z)\, dz \qquad \text{(S1)}$$

where ρ is the radial coordinate centered on the z axis, $z = 0$ is defined as the substrate surface, C is the concentration of calcein as a function of position and time (described below), and A is an unknown proportionality constant which includes such items as detector efficiency, filters, etc. $I_{laser}(z)$ is the intensity profile from TIRF excitation and is given as $I_{laser}(z) = I_0\, exp(-z/z_0)$, where z_0 is the characteristic decay length of the evanescent field (approximately 100 nm for our objective). ϕ_{rel} is the relative quantum yield of the calcein fluorophore. In their report, Weisshaar et al. (S2) present a method for empirically determining ϕ_{rel} by measuring the fluorescence intensity per molecule across a range of calcein solutions at various concentrations on their TIRF microscope. Their data fit to an exponential decay as $\phi_{rel} = e^{-59.5C(\rho,z,t)}$ and this empirically determined parameter was then used in Eq. S1. We performed a similar empirical fit using data collected on our TIRF microscope and found that our data fit to $\phi_{rel} = e^{-33C(\rho,z,t)}$.

Ultimately, the difference in decay constants made little difference to the normalized intensity calculation described below.

Depending on whether the calcein molecules are released under the DNA-tethered bilayer patch (content transfer) or above the patch (content leakage or bursting), the concentration C of the calcein molecules can be modeled according to either the 2D diffusion equation

$$C(\rho,t) = \frac{C_0 V_{ves}}{4\pi h D t} e^{-\rho^2/4Dt} \qquad \text{(S2)}$$

or 3D diffusion equation into a half-space

$$C(\rho,z,t) = \frac{2C_0 V_{ves}}{(4\pi D t)^{3/2}} e^{-(\rho^2+z^2)/4Dt} \qquad \text{(S3)}$$

where C_0 is the initial concentration of calcein fluorophores (100 mM for our experiments assuming 100% encapsulation efficiency) inside an SUV of volume V_{ves} (6.54×10^{-20} L for a 50 nm SUV) and D is the solution diffusion coefficient of a calcein molecule, which is the parameter varied to fit the data (described below).

Because we believed that an absolute fluorescence intensity calculation would be unproductive for our system, where many of the parameters in Eq. S1 are not known precisely, we opted to only examine the normalized integrated fluorescence intensity of each vesicle, using the time decay profile to distinguish between quasi-2D and 3D diffusion. In this case, the integrated fluorescence intensity is normalized as $F(t)_{normalized} = F(t)/\max(F(t))$ and the unknown (or imprecisely estimated) parameters of A, C_0, I_0, and V_{ves} are effectively canceled out when the calculation is performed.

Using MATLAB to perform the integrals numerically, we calculated $F(t)_{normalized}$ for each diffusion model using the values described above. For 2D diffusion, we used h_{2D} = 8 nm and integrated from z = 0 nm to $z = h_{2D}$, corresponding to diffusion between the underside of the membrane patch and the substrate. For the 3D diffusion model, we used h_{3D} = 4 μm and integrated from z = 8 nm to $z = h_{3D}$ corresponding to an SUV bursting above the membrane patch surface. By varying the parameters, we determined that $F(t)_{normalized}$ was most strongly dependent on which model was chosen for the analysis (2D or 3D diffusion) as well as the radius of analysis R, whereas significant variations in h, z_0, and the ϕ_{rel} decay constant had little effect on the overall time trace, as well as C_0 or V_{ves} as expected. We therefore used the above parameters in our curve fitting below.

As described in the manuscript text, the data of integrated fluorescence intensity time traces for SUVs fusing to tethered membrane patches were compiled from the raw image video streams using a homemade MATLAB program that integrated the calcein fluorescence inside a 4 μm radius circle centered on each vesicle for each video frame.

After a background subtraction, the integrated intensity time traces were normalized by dividing by the maximum integrated intensity value.

The data from each of these normalized integrated fluorescence intensity time traces could then be fit by the method of least squares to the 2D and 3D diffusion models described above to determine whether the SUV had fused to the membrane patch or had burst/leaked above the membrane patch. In the least squares fit (performed using home-written software in Matlab), the diffusion coefficient in each model was allowed to vary from 0 to 5000 μm^2/sec and the data was fit from t = 0 to t = 104.5 ms. Using the Stokes-Einstein equation, we expect that the solution diffusion coefficient of calcein should be ~200-400 μm^2/sec. Therefore, we looked not only for which model (2D or 3D) best fit the data, but also at the calculated value of the diffusion coefficient obtained from the fit.

Our data for the content transfer events was collected at 5.5 ms time resolution, and in order to account for the fact that content transfer could begin to occur at any point within that 5.5 ms window, we included in our fit a time offset parameter, which varied from 0 to 5.5 ms in 0.5 ms steps. At each iteration of the fit, the numerically integrated models were calculated at 0.5 ms time resolution and then combined into 5.5 ms bins in order to compute the least squares fit to the data. It is for this reason that the fits to the data (e.g. red and black lines in Figure 2 and Figure S1) are discretized.

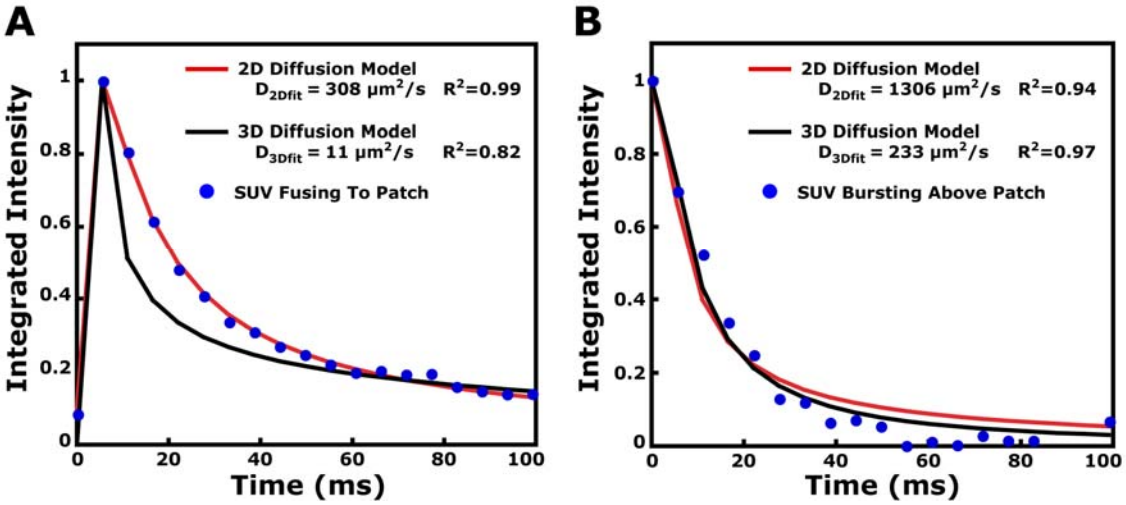

FIGURE S1. Example fits of the 2D (red line) and 3D (black line) diffusion models to the normalized integrated fluorescence intensity (blue circles) from two potential content transfer events of SUVs to a tethered bilayer patch. In (A) the 2D model fits the data much better and produces a more reasonable diffusion coefficient (308 μm^2/s) and so the event is identified as content transfer (i.e. fusion). In (B) both models fit the data, but only the 3D model yields a reasonable diffusion coefficient (233 μm^2/s), and so the event is identified as content bursting/leakage. These events were very rare (n=5 out of 125).

A least squares fit for each model (2D or 3D) was performed on the data from many potential content transfer events (n=125), excluding noisy events which were not fit well by either model ($R^2 < 0.86$ for both models) or events which occurred within 1-2 microns of the edge of the patch (to minimize edge effects). For each data time trace, the calculated diffusion coefficient for the 2D (D_{2Dfit}) and 3D (D_{3Dfit}) models were compared

following the fit. It was observed that the majority of the traces (n=111 of 125) fit well to the 2D diffusion model with diffusion coefficients (D_{2Dfit}) centered around 333 μm^2/sec. The fit of the 3D diffusion model for these traces proved too unrealistic—producing calculated 3D diffusion coefficients (D_{3Dfit}) in the tens of μm^2/sec (too slow for the diffusion of calcein into the bulk solution) and/or fitting the data poorly ($R^2 < 0.85$). Therefore, the 2D diffusion model was accepted for these traces, supporting the hypothesis that content transfer across the tethered bilayer patch and into the quasi-2D space beneath the patch had occurred for these events. An example comparison of the 2D and 3D least squares fit to one of these content transfer events is shown in Figure S1A. A histogram of the calculated 2D diffusion coefficients for all of the identified content transfer events is shown in Figure S2. The average diffusion coefficient for this population was 333 ± 117 μm^2/sec. We note that some of the calculated diffusion coefficients for this population are somewhat higher than expected and we suspect that this is due to the rapid photobleaching of the calcein dye following dequenching, which is not taken into account in the diffusion model and which would make the dye appear to diffuse faster than expected.

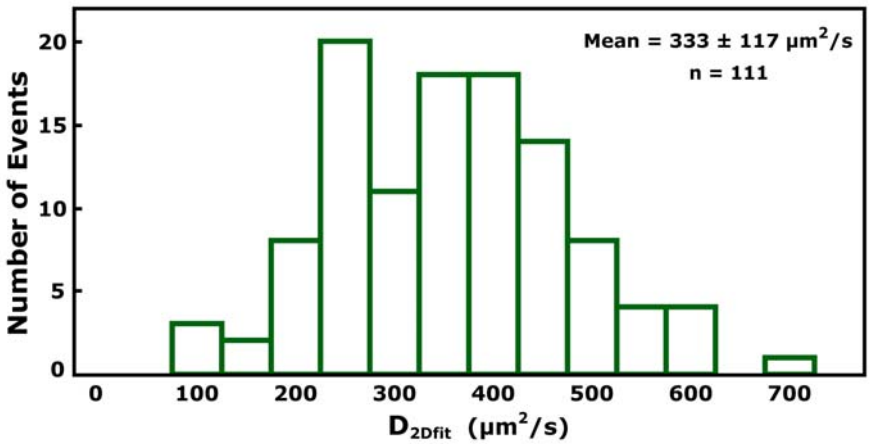

FIGURE S2. **Histogram of the calculated diffusion coefficients for all identified content transfer events (n=111) from the DNA-mediated SUV-to-tethered bilayer patch fusion experiments. The mean diffusion coefficient was 333 ± 117 μm^2/s (± 1 standard deviation).**

The normalized integrated intensity time traces of several potential content transfer events (n=5 of 125) were fit well by the 3D diffusion model and yielded reasonable diffusion coefficients (D_{3Dfit}) of ~130-230 μm^2/sec. The 2D diffusion model also fit these traces quite well, but with unreasonably high diffusion coefficients (D_{2Dfit}) of ~700-1300 μm^2/sec. Therefore, for these events, the 3D diffusion model was accepted, supporting the idea that the content had burst above the patch in these instances. An example trace of one of these events, overlaid with the least squares fit for both the 2D and 3D diffusion models is shown in Figure S1B.

The remaining events (n=9 of 125) were fit equally well by both the 2D and 3D diffusion models, with diffusion coefficients of ~100-130 μm^2/sec from the 3D fit and ~500-700 μm^2/sec from the 2D fit. In this case, neither model could be reliably accepted over the other and so this data was not assigned as either content transfer or content

bursting. It is possible that these traces represent events where both content transfer and bursting are occurring simultaneously (i.e. leaky fusion).

DOCKING TO FUSION TIMES FOR CONTENT TRANSFER EVENTS

The docking to fusion time was calculated for each of the SUVs which were determined to have undergone DNA-mediated fusion to the tethered bilayer as established by the diffusion analysis of the content dye described above (i.e. each of the events in Figure S2, excluding 3 events whose docking to fusion time could not be reliably determined). Docking was set at the video frame at which the SUV first appeared on the patch, detected by the faint residual fluorescence of the self-quenched calcein content dye. The fusion time was set at the frame in which content transfer was observed to begin. A histogram of the docking to fusion times for these events is shown in Figure S3. The majority of events are observed to have docking to fusion times of less than 1s, and a few events tail to much longer times (10-20 seconds). The average docking to fusion time for this population was 1.8 sec.

These docking to fusion times are much longer than what is typically observed in SNARE-mediated fusion experiments in live cells (ms timescale, see ref. S5) and that likely reflects differences between DNA-mediated fusion and the Ca^{2+}-triggered process of exocytosis.

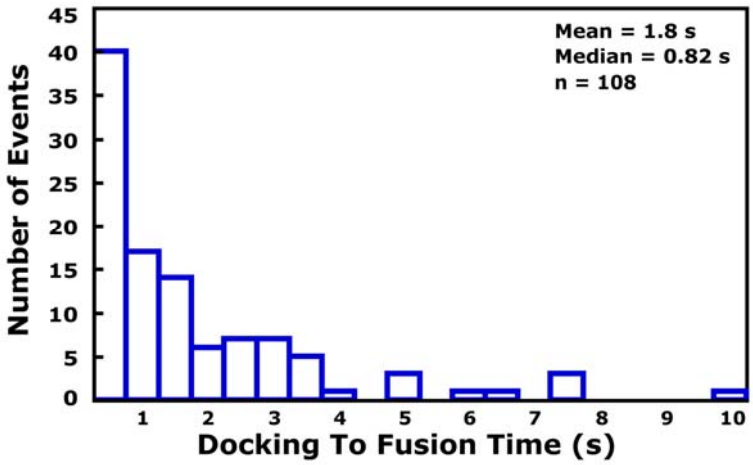

FIGURE S3. Histogram of the docking to fusion times of the observed content transfer events from the SUV-to-tethered bilayer fusion experiments. The average docking to fusion time is 1.8 s.

PARTIAL CONTENT TRANSFER

Approximately 12% of the content transfer events in the SUV-to-tethered bilayer patch fusion experiments were observed to undergo only partial content release and the ability to reliably detect such events is an exciting opportunity for membrane fusion studies on simple model systems. Movie S4 shows an example of a partial content transfer event and the time trace of the normalized integrated intensity for that event is shown below in Figure S4 (radius of integration = 4 μm). The SUV is observed to dock at t=350ms and undergoes slight photobleaching. At t=575ms, the content transfer event occurs. Because it is only a partial content transfer event, the normalized integrated

intensity does not decay to the zero baseline following content release and diffusion of the free dye out of the integration region.

Note that the self-quenched content dye inside the SUV exhibits two features that complicate further analysis of the time trace shown in Figure S4. First, photobleaching of the self-quenched dye between docking and content transfer must be occurring but does not cause the SUV to become brighter. This is either because a photobleached calcein dye molecule may still be able to quench other calcein molecules which are not yet photobleached, or because the level of photobleaching is insufficient to appreciably de-quench the trapped dye. Second, after partial content release, the normalized integrated intensity within the region of interest decays to a value similar to that before content release. We interpret this to mean that the remaining calcein molecules in the SUV following partial content release are now less self-quenched, and so even though fewer content dye molecules remain inside the SUV, the integrated intensity value is similar to that before content release. Since these experiments are designed to produce the largest possible increase in fluorescence upon content release, more quantitative analysis of these intermediate levels is not warranted.

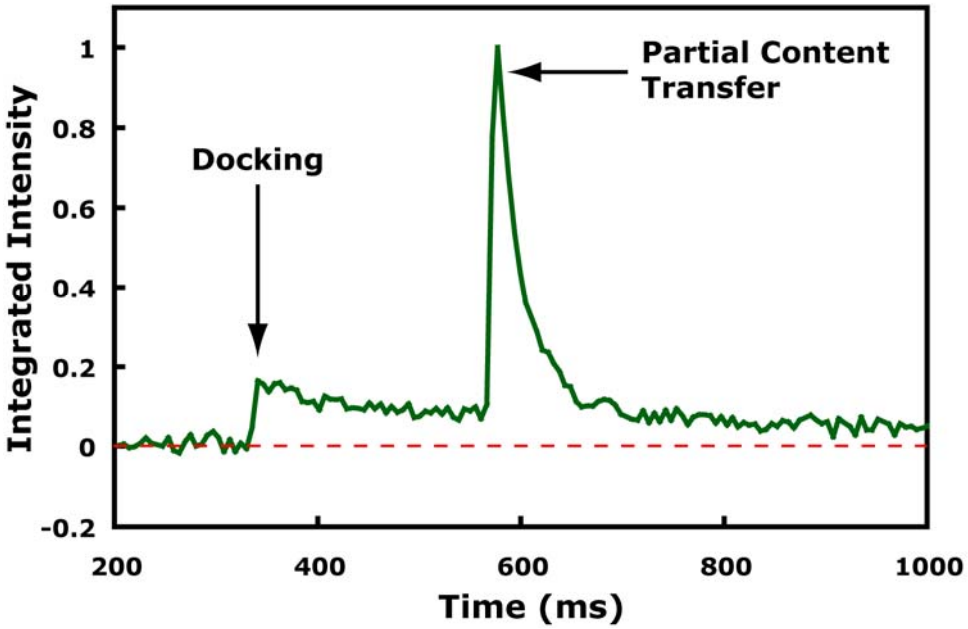

FIGURE S4. Example time trace (green) of the normalized integrated intensity (radius of integration = 4 μm) for a partial content transfer event, compiled from the event shown in Movie S4. The calcein-filled SUV docks at t = 350ms and a partial content transfer occurs at t =575ms. t=0 is set at the beginning of Movie S4. The zero baseline (red dashed line) is shown to emphasize that the integrated intensity does not decay to background following the partial content transfer.

CONTENT TRANSFER TO A TETHERED GUV

If the density of DNA-tethers between the substrate and the GUV is low enough, then the GUV does not rupture to form a tethered membrane patch, but instead remains intact on the surface, forming a flattened contact region where it is tethered to the surface, as shown in Figure S5A (S1). As with DNA-tethered bilayer patches, SUVs can fuse to

these tethered GUVs by DNA-mediated fusion (schematically shown in Figure S5B) and although the tethered GUVs are considerably more fragile than the robust tethered membrane patch system, content transfer can be clearly observed.

To observe DNA-mediated content transfer to a tethered GUV, we prepared a tethered GUV system as follows. An immobilized DNA surface was prepared as before, but with a much lower density of tethers (Sequence 2, Supplementary Table 1) by reducing the concentration of alkyne-modified DNA or the amount of time the click reaction was allowed to occur (~15 min instead of the usual 90 min). GUVs were prepared by electroformation as previously described (S1). The lipid mixture for the GUVs was 2:1:1 DOPC:DOPE:chol, 0.2 mol% DiD lipid dye, and 0.5 mol% each of Sequence 1 and PolyT-lipid (see Supplementary Table 1). The lipid mixture was dissolved in methanol and coated on platinum electrodes to form a dried lipid film. Electroformation was performed at 2.5V and 10Hz for a minimum of 90 minutes at 60 C in a 0.5 M sucrose solution. The vast majority of GUVs obtained with this method are unilamellar, a requirement for a content transfer experiment to an intact GUV.

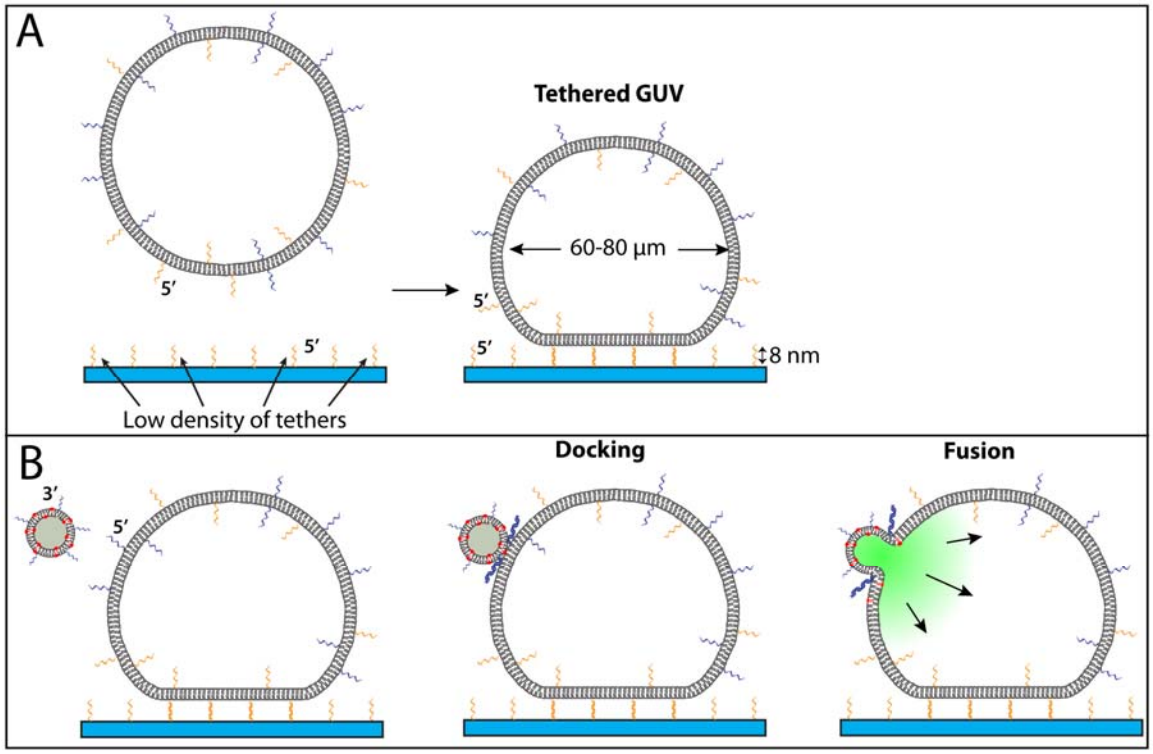

FIGURE S5. (A) Schematic depicting the formation of a DNA-tethered GUV. If the density of DNA tethers on the substrate is low enough, then the GUV does not rupture to form a tethered bilayer patch, but remains intact on the surface, forming a flattened contact region where it is tethered to the surface. (B) Schematic of DNA-mediated fusion of an SUV to a tethered GUV. The SUV is filled with a self-quenched concentration of content dye, and upon DNA-mediated content transfer, dequenching occurs, producing a fluorescent burst into the interior of the GUV. Note that while this provides a compelling visualization of the sidedness of content release, it can not be further quantified as the location of the focal plane of the event is not characterized, in contrast to the TIR measurements of dye release beneath a tethered membrane patch or for an SUV bursting on a surface.

After electroformation, GUVs were added to the immobilized DNA surface. Once a sufficient population of GUVs was tethered to the surface, excess GUVs were removed from the bulk solution by very gentle rinsing. A suitable tethered GUV was localized by epifluorescence microscopy and then several μL of a diluted SUV suspension were manually pipetted into the solution above the tethered GUV. SUVs for this experiment contained 125mM self-quenched calcein, 0.1% DiI lipid dye, and displayed 0.5 mol% PolyA-lipid. After a short time, SUVs were observed to have accumulated on the domed surface of the tethered GUV and content transfer events into the interior of the tethered GUV were captured with epifluorescence microscopy (Movie S2). Content transfer to the GUV resulted in dequenching of the calcein content dye, producing a bright "explosion" of fluorescence into the GUV which quickly expanded to fill the volume enclosed by the GUV. Frame snapshots of one content transfer event from Movie S2 are shown in Figure S6. As mentioned in the main text, we highlight that these content transfer events to a tethered GUV unambiguously demonstrate content transfer into a confined space. However, quantitative diffusion analysis (as was done for the tethered patch system) is not possible because the analysis requires knowledge of the location of the focal plane relative to the fusing SUV, and for the tethered GUV system the event must be captured via epifluorescence rather than TIRF illumination and the exact vertical location of the SUV on the surface of the GUV is not known.

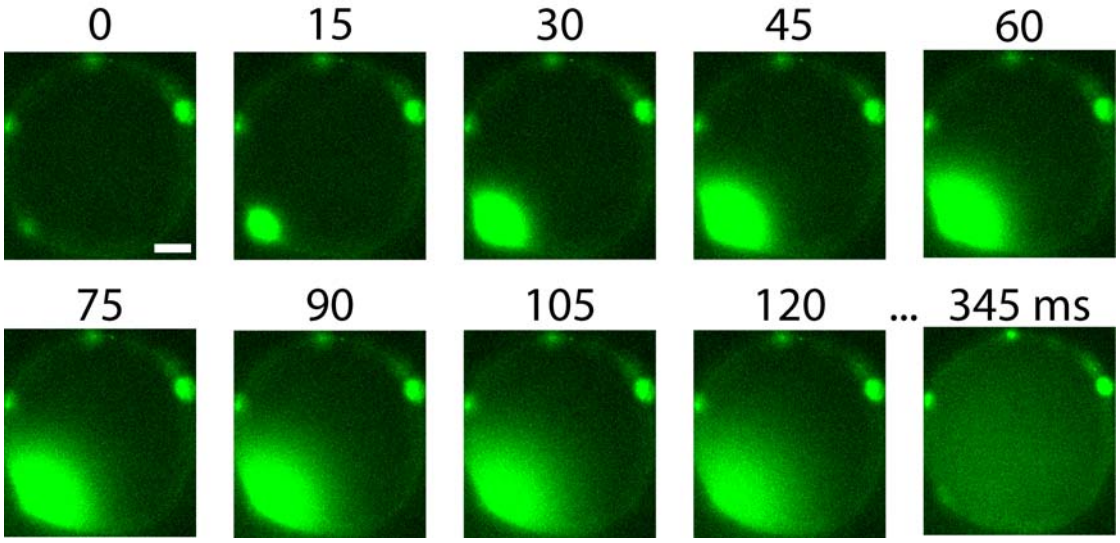

FIGURE S6. Frame snapshots from Movie S2 showing a content transfer event from a calcein-filled SUV to a tethered GUV by DNA-mediated membrane fusion. t=0 is set at the frame before the fusion event occurs. The scale bar (in the t=0 frame) is 6 μm.

CONTENT TRANSFER TO A LIPID TUBULE

During the formation and rinsing of a DNA-tethered bilayer patch, lipid tubule structures can be pulled from the edge of the patch and are observed to adhere stably to the substrate (see Figure S7). These lipid tubule structures are ill-defined and of unknown radii. However, during typical SUV fusion-to-patch experiments, SUVs can be observed to both dock and fuse to lipid tubules that are located nearby the tethered patch being observed. Content transfer to these structures is clearly observed, as the de-quenching fluorescent content dye spreads quickly along tubule structure and not into the

surrounding solution. Movie S3 shows a content transfer event into a lipid tubule located nearby a tethered bilayer patch to which SUVs are docking and fusing. Content transfer events to lipid tubules are not useful for quantitative experiments, because the nature of the tubule is so ill-defined. However, as with content transfer to a tethered GUV, content transfer to a lipid tubule unambiguously demonstrates that fusion has occurred because the content dye has been transferred into an enclosed space.

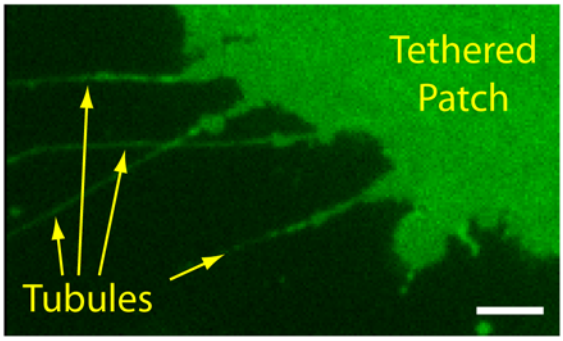

FIGURE S7. Epifluorescence image of the edge of a DNA-tethered bilayer patch from which lipid tubules have been pulled. The tubules were created during formation and rinsing of the tethered patch and are now stably attached to the substrate surface. The scale bar is 4 μm.

DIFFUSION ANALYSIS OF LIPID-MIXING

If content transfer is truly occurring in the SUV-to-tethered bilayer fusion experiments, then we should observe a large difference between the speed at which the content dye diffuses outward in the 8nm gap underneath the tethered bilayer and the speed at which the lipid dyes diffuses outward in the bilayer. To quantify this difference, we performed a diffusion analysis on many lipid-mixing events (n=168) at 53 ms time resolution and compared the calculated diffusion coefficients for the lipid dye (Figure S8B) to those calculated for the content dye (Figure S2).

For each lipid-mixing event, the normalized integrated fluorescence intensity within a 2.2 μm radius was calculated at each time step in a video stream using a homemade Matlab program. t=0 was set at the time point in which lipid-mixing to the tethered bilayer began to occur. The data was then fit using a least squares method to the numerically integrated 2D diffusion equation (Eq. S2) to obtain a calculated diffusion coefficient D_{2Dfit}. An example fit is shown in Figure S8A (note that the appropriate model for this fit is the integrated 2D diffusion equation (Eq. S2) and not the model used for the analysis of the content transfer data (Eq. S1) which contains terms to account for dequenching as well as diffusion).

A histogram was compiled for the calculated 2D diffusion coefficients of many lipid-mixing events (n=168). The mean diffusion coefficient for the data was 4.1 ± 1.4 μm^2/sec, consistent with the diffusion coefficient of a lipid dye in a tethered bilayer patch previously measured by fluorescence recovery after photobleaching (FRAP) (S1). The

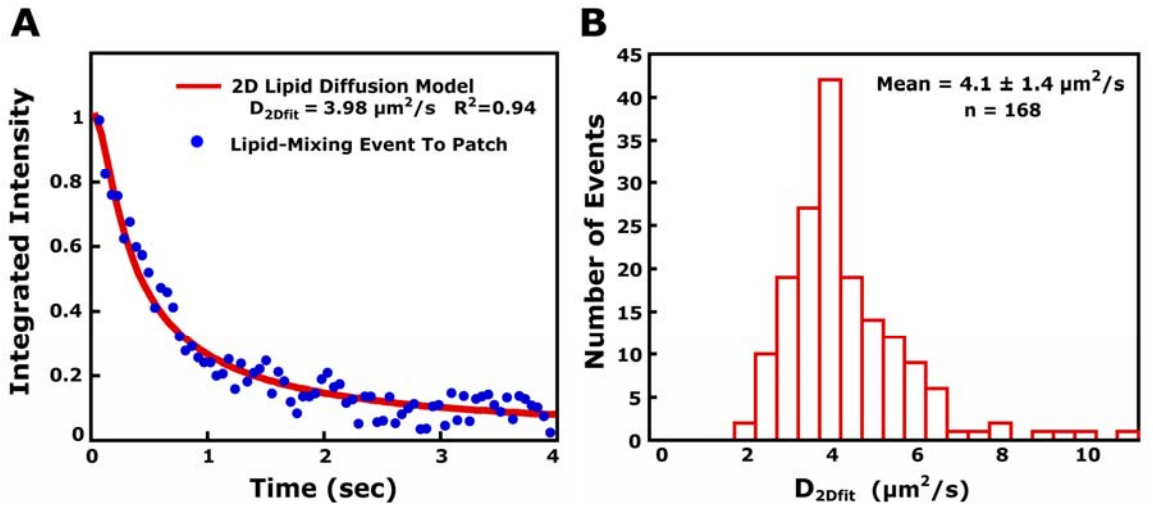

FIGURE S8. (**A) Example fit (red line) of the 2D diffusion equation (Eq. S2) to the normalized integrated fluorescence intensity time trace (blue circles) collected from a lipid-mixing event of an SUV fusing to a tethered bilayer patch. Radius of integration was 2.2 μm. (B) Histogram of the diffusion coefficients calculated from fitting the integrated intensity data of many lipid-mixing events (n=168). The mean diffusion coefficient was 4.1 ± 1.4 μm²/s (± 1 standard deviation).**

large difference between the average diffusion coefficient of the lipid dye (4.1 ± 1.4 μm^2/sec) and the content dye (333 ± 117 μm^2/sec) is consistent with the assertion that fusion (both lipid-mixing and content transfer) is occurring in the DNA-mediated SUV-to-tethered bilayer fusion experiments. In contrast to content transfer, the efficiency of lipid-mixing is very high—approximately 60-80% of SUVs are observed to undergo lipid-mixing at the DNA-lipid concentrations used in this study (0.75-1 mole %) over the timescale of a typical experiment (~90 sec). Most of the observed lipid-mixing events are hemi-fusion.

NOTE ON LIGHT-INDUCED VESICLE FUSION

The purpose of this letter is to present our observation of content transfer across a free-standing membrane patch, which sets the stage for parallel measurements using SNAREs, and not to discuss in-depth the mechanism of DNA-mediated vesicle-to bilayer patch fusion. We include here, however, a cautionary word about the effects of light levels on the time between docking and fusion for this and other fluorescence-based vesicle fusion experiments.

During content transfer experiments as described above in which the docking to fusion time was measured, it was observed that the average time between an SUV docking to the tethered bilayer and when it underwent content transfer exhibited a strong dependence on the intensity of the light used to collect the data. As the light intensity increased, the time between docking and fusion was greatly diminished, indicating that the light was facilitating vesicle fusion to some degree. Light alone was not sufficient to produce vesicle fusion or leakage, as indicated by the fact that vesicles docked to the membrane patch in a tethering orientation (i.e. with a ~8nm "rigid rod" hybridized 24mer between the patch and vesicle) rather than the fusing orientation shown in Figure 1, were

not observed to undergo content transfer or bursting, regardless of the light level. The Brunger lab has previously reported light-induced SNARE-mediated fusion of calcein-filled vesicles, and identified local heating from the incident laser light as the mechanism of the light-induced fusion (S4). Our study into this issue using DNA-mediated fusion has indicated that this problem is not specific to calcein. Indeed, two separate content dyes (calcein and sulforhodamine B) and one lipid-mixing dye (Texas Red-DHPE) at a variety of concentrations all exhibited shorter docking to fusion times at higher incident light intensities. Not surprisingly, self-quenched content dyes, where the energy from absorbed light is more likely to be dissipated as heat because relaxation by fluorescence is greatly reduced, exhibited this behavior to a greater extent than the lipid-mixing dye, which was not self-quenched.

Therefore, we suggest that caution should be employed with respect to incident light intensity when collecting vesicle fusion data using fluorescence microscopy, not only for our system, but for any fluorescence-based single vesicle fusion assay. It is recommended that data collected at different light levels be compared to ensure that the incident light intensity is not affecting the timescales of docking to fusion. In our system, we observed that the docking to content mixing time seems to depend more heavily on light levels than the docking to lipid-mixing time. Indeed, it appears as though our DNA-mediated fusion system transitions easily to a hemi-fusion intermediate on the order of seconds, while content transfer happens much more slowly and infrequently, on the order of tens of seconds to minutes, unless a high level of light is employed to facilitate a faster transition to content transfer.

SUPPORTING MOVIE INFORMATION

Movie S1. A docking and fusion event of a calcein-filled SUV to a tethered bilayer patch, visualized by TIRF microscopy. The frame rate has been slowed ~6x to facilitate viewing. The total real time of the movie is 0.5 sec.

Movie S2. Several fusion events of calcein-filled SUVs to a tethered GUV, visualized by epifluorescence microscopy. In the movie, the focal plane is passed up and down through the "dome" of the tethered GUV and content transfer into the enclosed space of the GUV is observed. The frame rate has been slowed ~2x to facilitate viewing. The total real time of the movie is 4.5 sec.

Movie S3. A fusion event of a calcein-filled SUV to a V-shaped lipid tubule, visualized by TIRF microscopy. Several content transfer events due to SUVs fusing to a nearby tethered bilayer patch are also shown. The frame rate has been slowed ~6x to facilitate viewing. The total real time of the movie is 0.8 sec.

Movie S4. A docking and partial content transfer event of a calcein-filled SUV to a tethered bilayer patch, visualized by TIRF microscopy. The frame rate has been slowed ~6x to facilitate viewing. The total real time of the movie is 1.7 sec.

SUPPORTING REFERENCES

S1) Chung, M., Lowe, R. D., Chan, Y-H. M., Ganesan, P. V., and S. G. Boxer. 2009. DNA-tethered membranes formed by giant vesicle rupture. *J. Struct. Biol.* 168:190-199.

S2) Wang, T., Smith, E. A., Chapman, E. R., and J. C. Weisshaar. 2009. Lipid Mixing and Content Release in Single Vesicle, SNARE-Driven Fusion Assay with 1-5 ms Resolution. *Biophys. J.* 96: 4122-4131.

S3) Chan, Y-H. M., van Lengerich, B., and S. G. Boxer. 2008. Lipid-anchored DNA mediates vesicle fusion as observed by lipid and content mixing. *Biointerphases*. 3:FA17-FA21.

S4) Bowen, M. E., Weninger, K., Brunger, A. T. and S. Chu. 2004. Single Molecule Observation of Liposome-Bilayer Fusion Thermally Induced by Soluble N-Ethyl Maleimide Sensitive-Factor Attachment Protein Receptors (SNAREs). *Biophys. J.* 87: 3569-3584.

S5) Ge, S., S. Koseoglu, and C.L. Haynes. 2010. Bioanalytical tools for single-cell study of exocytosis. Anal. Bioanal. Chem. 397:3281-3304.